

## Order-disorder effects in the phase transitions of $\text{LiNbO}_3$ and $\text{LiTaO}_3$ measured by perturbed-angular-correlation spectroscopy

Gary L. Catchen and David M. Spaar\*

*Department of Nuclear Engineering and Materials Research Laboratory, The Pennsylvania State University, University Park, Pennsylvania 16802*

(Received 10 June 1991)

Perturbed-angular-correlation (PAC) spectroscopy was used to measure nuclear-electric-quadrupole interactions at the Li sites in two isostructural, ferroelectric ternary-metal oxides,  $\text{LiNbO}_3$  and  $\text{LiTaO}_3$ . These compounds were prepared as ceramics doped with approximately 0.01 at. % Hf that carried the radioactive  $^{181}\text{Hf} \rightarrow ^{181}\text{Ta}$  PAC probes. PAC measurements were made over a temperature range from 295 to  $\approx 1100$  K, which included the ferroelectric-to-paraelectric transition for  $\text{LiTaO}_3$ . Because the transition temperature  $T_c$  for  $\text{LiNbO}_3$  exceeded the accessible temperature range of the available apparatus, the investigation focused mainly on the features of the  $\text{LiTaO}_3$  transition. In particular, the measured perturbation functions show well-defined, high-frequency, static interactions that are characterized by extensive line broadening at temperatures well below  $T_c$  and by significantly less line broadening at temperatures above  $T_c$ . At temperatures above  $T_c$ , the electric-field-gradient (efg) asymmetry parameter  $\eta$  is close to zero, but at temperatures well below  $T_c$ ,  $\eta$  is significantly larger than zero. This result is not expected, because the axial symmetry at the Li site associated with the diffraction-derived structure implies that  $\eta$  should vanish at temperatures both below and above  $T_c$ . The observed  $\eta$  temperature dependence is explained using an order-disorder model. This model suggests that some of the Li ions (and to some extent group-V antisite defects) occupy normally vacant metal sites and break the axial symmetry associated with the Li site. At temperatures below  $T_c$ , the efg component  $V_{zz}$  increases as temperature increases, and over the same temperature range, the spontaneous polarization decreases. For this reason,  $V_{zz}$  may not be strongly coupled to the order parameter for the transition. However, the anomalous temperature dependence of  $\eta$  suggests that  $\eta$  may be coupled to the order parameter.

### I. INTRODUCTION

Lithium niobate,  $\text{LiNbO}_3$ , is a well-known ferroelectric material that has many applications to the technology of piezoelectric, optical, and electrical-optical materials and devices. Lithium tantalate,  $\text{LiTaO}_3$ , is an isostructural material that has similar physical properties. Since the 1960's, when the structures were determined,<sup>1,2</sup> these materials have been investigated extensively by many techniques. Moreover, the literature contains several thousand papers published on  $\text{LiNbO}_3$  and  $\text{LiTaO}_3$ .<sup>3,4</sup> Despite the myriad of studies, the phase-transition mechanisms remain unclear. One particular open question is whether the ferroelectric-to-paraelectric transitions are either displacive or order-disorder in character. The purpose of this investigation is to use PAC spectroscopy via the  $^{181}\text{Hf} \rightarrow ^{181}\text{Ta}$  probe to clarify which of these phase-transition mechanisms is operative.

These materials, which each undergo a single, second-order ferroelectric-to-paraelectric transition,<sup>3</sup> have ilmenitelike structures that belong to the  $R3c$  and  $R\bar{3}c$  space groups at temperatures below and above the transition temperature, respectively. In this structure, the metal ions occupy sites that have octahedral oxygen coordination, and one third of these octahedral sites are vacant. These vacant sites potentially can give rise to disordering when Li ions occupy some of them. The transition temperatures  $T_c$  are among the highest known for ternary-

metal oxide ferroelectrics,  $\approx 1480$  K for  $\text{LiNbO}_3$  and  $\approx 950$  K for  $\text{LiTaO}_3$ . Because  $T_c$  is so high for  $\text{LiNbO}_3$  and because the melting point is only about 50 K higher, the transition is experimentally difficult to study. Furthermore, the transition temperatures and other physical properties differ depending on whether crystals of these materials are prepared that have either the congruent-melting composition, which is several percent deficient in Li, or the stoichiometric composition.

During the last three decades, nuclear quadrupole interactions at the Li and the group-V sites have been measured using nuclear magnetic resonance (NMR), nuclear quadrupole resonance (NQR), and Mössbauer-effect (ME) spectroscopies. The most extensively used technique has been NMR spectroscopy, which can measure nuclear quadrupole interactions via the resonant transitions of  $^7\text{Li}$  ( $I = \frac{3}{2}$ ) and  $^{93}\text{Nb}$  ( $I = \frac{9}{2}$ ) nuclei.<sup>5-15</sup> These investigations have been performed primarily at laboratory temperature on both single-crystal and powder specimens. In the earliest experiments, the quadrupole coupling constant,  $\nu_Q = e^2qQ/h$  ( $eq = V_{zz}$ ), was measured at the Li sites in  $\text{LiNbO}_3$  (Ref. 5) and  $\text{LiTaO}_3$  (Refs. 5-7) and at the Nb site in  $\text{LiNbO}_3$ .<sup>6,7</sup> An objective of the earliest of these investigations<sup>5</sup> was to correlate the change of the Li quadrupole coupling constant with temperature with the corresponding changes in the spontaneous polarization  $P_s$ . These results could not be interpreted properly because they were compared to the original report of the

spontaneous polarization<sup>16</sup> that erroneously showed an increase in  $P_s$  with temperature.<sup>17</sup> A primary contribution of the later two experiments,<sup>6,7</sup> was to characterize the metal-oxygen bonding in terms of covalency. Although these investigations did show that  $\text{LiNbO}_3$  and  $\text{LiTaO}_3$  are highly covalently bonded crystals, they assumed that the electric-field-gradient (efg) at both metal sites had axial symmetry, because the derived crystal structures<sup>1,2</sup> had threefold rotational axes that ran through the metal sites. In the later experiments,<sup>8,10</sup> broadening of the NMR line shape was used to measure small changes in the Li composition that characterized melt-grown crystals of  $\text{LiNbO}_3$ . These investigations, which contributed to establishing the phase diagram of  $\text{LiNbO}_3$ , demonstrated that the nuclear quadrupole interaction as measured by NMR spectroscopy is sensitive to the effects of defects in  $\text{LiNbO}_3$  and  $\text{LiTaO}_3$ . More recently,  $^{93}\text{Nb}$  NMR measurements were performed on  $\text{LiNbO}_3$  ceramic samples.<sup>11</sup> These measurements showed extensive spectral line broadening, and this feature was attributed to Lorentzian distributions of quadrupole coupling constants that Li deficiencies produced.<sup>11</sup> Douglass, Peterson, and McBrierty<sup>12</sup> extended the earlier single-crystal measurements<sup>8,10</sup> and developed a more sophisticated model with which the effects of defects and nonstoichiometry on the NMR line shape could be interpreted. In addition NMR measurements performed on ceramic samples of the  $\text{LiNbO}_3$ - $\text{LiTaO}_3$  solid-solution system<sup>13</sup> showed that the spectral linewidth magnitudes correlated with the extent of the random distribution of the group-V ions in the crystal. The linewidths were largest for solid solutions that had nearly equal concentrations of Nb and Ta. To investigate Li-ion motion, elevated-temperature  $^7\text{Li}$  NMR experiments were performed on a  $\text{LiNbO}_3$  single crystal.<sup>14</sup> The quadrupole coupling constants were found to increase linearly with temperature. This temperature dependence was attributed to the anisotropic vibrational motions of the Li ions. The spectral linewidths were found to be large at lower temperatures and to decrease nonlinearly with increasing temperature. The line broadening observed at lower temperatures was attributed to Li ions hopping between the normal Li sites and the vacant sites. The complete motional narrowing observed at higher temperatures was attributed to Li-ion diffusion. In a later investigation of Li-ion motion,<sup>15</sup> the spin-lattice relaxation time  $T_1$  of  $^7\text{Li}$  in  $\text{LiTaO}_3$  powder was measured at elevated temperatures. The relaxation observed at lower temperatures was attributed primarily to the effects of paramagnetic impurities. The  $T_1$  temperature dependence was discussed in the context of a diffusion mechanism, in which the Li ions jump from the normal Li sites to interstitial sites. The observed relaxation was explained by the diffusing Li ions coupling to the lattice via the nuclear quadrupole interaction. Interestingly, the investigators<sup>15</sup> suggested that the Li-site efg couples to the order parameter for the ferroelectric-to-paraelectric transition in  $\text{LiTaO}_3$ .

Schempp, Peterson, and Carruthers<sup>18</sup> used  $^{93}\text{Nb}$  NQR spectroscopy to investigate powder samples of  $\text{LiNbO}_3$  over a temperature range from 21 to 515 K.

Stoichiometric samples gave reasonably sharp lines that yielded well-defined interaction frequencies. These measured frequencies were consistent with a small but nonvanishing asymmetry of the efg at the Nb site. Over the temperature range from laboratory temperature to 515 K, the quadrupole coupling constant decreased with increasing temperature. Samples that were deficient in Li gave highly broadened lines that did not yield discernible frequencies. Zhukov *et al.*<sup>19</sup> used  $^{181}\text{Ta}$  NQR spectroscopy to investigate ceramic samples of  $\text{LiTaO}_3$  over a temperature range from 77 K to laboratory temperature. They observed that, at the Ta site, the quadrupole coupling constant decreased with increasing temperature and that the efg asymmetry was small but nonvanishing.

Using  $^{181}\text{Ta}$  ME spectroscopy, Löhnert *et al.*<sup>20</sup> investigated a polycrystalline absorber of  $\text{LiTaO}_3$  over a temperature range from 4 to 1100 K. These measurements yielded the signed largest component  $V_{zz}$  and the asymmetry  $\eta$  of the efg at the Ta site. As temperature increased,  $V_{zz}$  was positive and decreased rapidly, and  $V_{zz}$  changed sign near 800 K. As temperature increased to about 800 K,  $\eta$  was small,  $<0.1$ , and increased to  $\approx 0.4$ ; and above 800 K,  $\eta$  decreased to a small value at 1100 K. In addition the measured magnitudes of  $V_{zz}$  and  $\eta$  agreed with those that Zhukov *et al.*<sup>19</sup> reported. Löhnert *et al.*<sup>20</sup> realized that the nonvanishing Ta-site efg asymmetry was inconsistent with the diffraction-derived structure symmetries both below and above  $T_c$ , since in both structures the Ta sites lie on axes of threefold rotation. But they did not attribute the unexpected, anomalous asymmetry-parameter values to a specific mechanism.

In the  $^{93}\text{Nb}$  NMR measurements on  $\text{LiNbO}_3$ , line broadening correlates with small changes in the Li composition away from stoichiometry. The broadening arises because some of the Nb nuclei may be either at Li sites (as antisite defects) or at Nb sites that have defects nearby. This interpretation of the line-broadening information has been very useful for measuring the effects of Li composition on phase equilibria. However, this NMR technique is not well suited to making elevated-temperature measurements, to investigate, for example, order-disorder effects at temperatures near  $T_c$ . Although the  $^{93}\text{Nb}$  NQR technique has been used for making elevated-temperature measurements<sup>18</sup>, the technique is not sensitive enough for investigating phase transitions in nonstoichiometric samples of  $\text{LiNbO}_3$ . Although the  $^{181}\text{Ta}$  ME technique is very sensitive to changes in the local efg near the Ta site in  $\text{LiTaO}_3$ , it cannot be used to study  $\text{LiNbO}_3$ . Similarly, out of these techniques, only  $^7\text{Li}$  NMR spectroscopy can be applied directly to investigate both  $\text{LiNbO}_3$  and  $\text{LiTaO}_3$ , but the sensitivity of the technique is limited by a small quadrupole coupling constant of the  $^7\text{Li}$  nucleus  $<100$  kHz.

Although NMR, NQR, and ME spectroscopies have provided much useful information about the local efgs at either one or both of the metal sites in  $\text{LiNbO}_3$ , none of these techniques can be used to measure the efgs at the *same* site in both compounds over a large temperature range. This type of measurement is necessary to characterize the associated phase-transition mechanism. Now

PAC spectroscopy can be used for the purpose of measuring the efgs at the same site in both compounds. Moreover, the PAC technique offers several advantages: (1) the PAC technique is very sensitive to the nuclear quadrupole interaction and measures it directly, (2) elevated-temperature measurements generally are not complicated by hardware external to the sample such as a large magnet, and (3) the  $^{181}\text{Hf} \rightarrow ^{181}\text{Ta}$  probe should substitute into the same site in both  $\text{LiNbO}_3$  and  $\text{LiTaO}_3$ . [The specific probe site depends on the chemistry of the  $^{181}\text{Hf}$  probe; whereas, the  $^{181}\text{Ta}$  excited ( $I = \frac{5}{2}$ ) level, which has a half life of 10.8 nsec, interacts with the efg at the probe site.] Because the PAC technique has these advantages, we embarked on a systematic study of the ferroelectric-to-paraelectric phase transitions in ceramic samples of  $\text{LiNbO}_3$  and  $\text{LiTaO}_3$ .

Specifically, we used the  $^{181}\text{Hf} \rightarrow ^{181}\text{Ta}$  PAC probe to measure nuclear quadrupole interactions at the Li sites in  $\text{LiNbO}_3$  and  $\text{LiTaO}_3$  over a temperature range from 295 to 1100 K. Although we did not have the capability to investigate the ferroelectric-to-paraelectric transition in  $\text{LiNbO}_3$ , we did investigate the transition in  $\text{LiTaO}_3$ . We interpret the measurements of the temperature dependences of the efg parameters  $V_{zz}$  and  $\eta$  and the line-shape parameters in the context of an order-disorder model.

## II. EXPERIMENTAL DETAILS

### A. Sample preparation

Ceramic samples of  $\text{LiNbO}_3$  and  $\text{LiTaO}_3$  were prepared using a variation of the resin-intermediate method, in which batches of approximately 3 g of product were prepared. To a solution of citric acid and ethylene glycol, the precursors,  $\text{LiNO}_3$  powder and solutions of either  $\text{Nb}(\text{OCH}_2\text{CH}_3)_5$  or  $\text{Ta}(\text{OCH}_2\text{CH}_3)_5$ , were added. Then approximately 30–60  $\mu\text{Ci}$  of the radioactive  $^{181}\text{Hf}$  probe was added to the solution as several milligrams of  $\text{HfOCl}_2$  dissolved in  $\text{H}_2\text{O}$ . The nominal Hf concentrations were approximately 0.01 at. % of the metal-ion concentrations. The solution was heated on an electric hot plate until a thick resin was formed. Then the resin was pyrolyzed. The residue was calcined in a box furnace at approximately 1000 K for 12 h, and the resulting metal-oxide powder was pressed into small pellets (approximately 7 mm in diameter and 4 mm thick) and sintered in air in a tube furnace at 1400–1600 K for 24 h. To check the sample phase purity, x-ray powder diffraction patterns were measured on small amounts of radioactive powder taken from the PAC samples. Figure

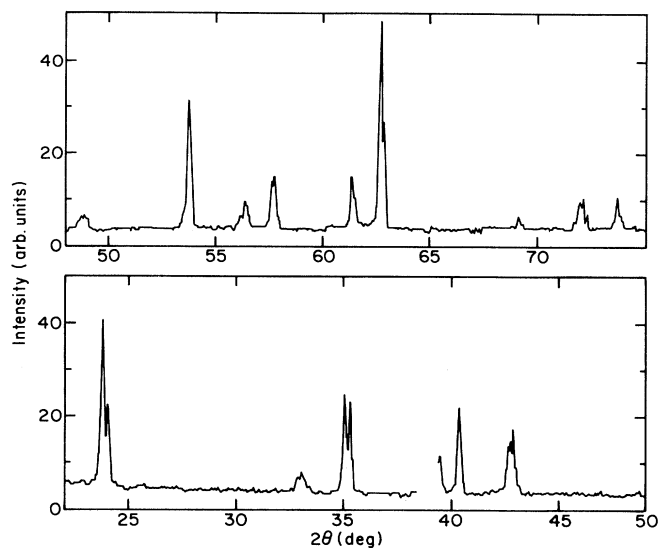


FIG. 1. X-ray powder diffraction pattern measured on a sample of  $\text{LiTaO}_3$ .

1 presents a typical pattern for  $\text{LiTaO}_3$ . To perform the PAC measurements, ceramic pellets that typically contained 15–30  $\mu\text{Ci}$  of  $^{181}\text{Hf}$  activity were sealed in fused-silica tubes. A simple tube furnace was used to maintain the elevated temperatures during the PAC measurements. Because the temperature control was simple, temperature drifts of 5–10 K during the measurement periods of 1–2 days were observed.

### B. PAC measurements

A recent paper presents most of the experimental details.<sup>21</sup> We present the relevant details here. A four-CsF-detector PAC apparatus, which has a time resolution of  $\approx 1$  nsec, full width at half maximum, was used to collect eight (four  $90^\circ$  and four  $180^\circ$ ) coincidences concurrently. The experimental perturbation functions  $A_{22}G_{22}(t_i)$  were obtained from the measured correlation functions  $W_{jk}(\theta_{jk}, t_i)$  that represented the primary experimental data (the subscripts  $j$  and  $k$  refer to the coincidence between the respective detectors, and  $i$  refers to the time interval). Specifically the ratio method was used to obtain  $A_{22}G_{22}(t_i)$ , which Eqs. (1) and (2) in Ref. 21 describe. To analyze the measured perturbation functions, a one-site model for nuclear electric quadrupole interactions in a polycrystalline source was used:

$$-A_{22}G_{22}(t_i) = A_1 \left[ S_0(\eta) + \sum_{k=1}^3 S_k(\eta) \exp\left(-\frac{1}{2}\delta\omega_k t_i\right) \cos(\omega_k t) \right] + A_2. \quad (1)$$

Here  $A_1$  is the normalization factor,  $\delta$  is the line-shape parameter, which is a measure of the relative width of the Lorentzian frequency distribution (of the  $\omega_k$ 's) that gives rise to static line broadening, and  $A_2$  takes into account

the effects of  $\gamma$  rays that are absorbed by the sample and the effects of the fraction of probe atoms that are not in a well-defined chemical environment, i.e.,  $A_2$  represents in part the “hard core” to which the corresponding pertur-

bation function decays. The frequencies  $\omega_k$  and the  $S_i(\eta)$  coefficients describe a static interaction in a polycrystalline source. Using nonlinear regression, the free parameters  $\omega_1$ ,  $\omega_2$ ,  $A_1$ ,  $A_2$ , and  $\delta$  were derived from each measured perturbation function. The ratio  $\omega_2/\omega_1$  was used to determine the quadrupole frequency  $\omega_Q$ , which is  $\omega_1/6$  when  $\eta=0$ .<sup>22</sup> The nonvanishing efg components  $V_{ii}$  in the principal-axis system where the probe nucleus is at the origin are related to the quadrupole frequency  $\omega_Q$  and the asymmetry parameter  $\eta$  by  $\omega_Q = [eQV_{zz}/4I(2I-1)\hbar]$  and  $\eta = (V_{xx} - V_{yy})/V_{zz}$ , in which  $Q$  is the nuclear quadrupole moment (2.51  $b$ ) of the spin  $I = \frac{5}{2}$  intermediate nuclear level in the  $^{181}\text{Ta}$  probe nucleus. The quadrupole coupling constant  $\nu_Q$  is related to the quadrupole frequency by  $\omega_Q = 2\pi\nu_Q/4I(2I-1)$ . In addition, the site-occupancy fraction  $f_1$  for the primary probe site is given by  $f_1 = A_1/(A_1 + A_2)$ .

### III. RESULTS

Figures 2 and 3 present several perturbation functions for  $\text{LiNbO}_3$  and  $\text{LiTaO}_3$ , respectively. Since  $T_c \approx 950$  K for  $\text{LiTaO}_3$ , several measurements were made above  $T_c$ . But, for  $\text{LiNbO}_3$ ,  $T_c \approx 1480$  K, and the furnace in use at the time could not reach temperatures above  $T_c$ . As a result we have no data for  $\text{LiNbO}_3$  at temperatures above  $T_c$ . Equation (1) was used to fit the experimental perturbation functions. Qualitatively, at temperatures below  $T_c$ , the perturbation functions for  $\text{LiNbO}_3$  and  $\text{LiTaO}_3$  are very similar in shape. This observation is consistent with the idea that the two compounds are isostructural. For both  $\text{LiNbO}_3$  and  $\text{LiTaO}_3$ , the perturbation functions measured at lower temperatures show extensive line broadening. For the  $\text{LiTaO}_3$  perturbation functions measured above  $T_c$ , the line broadening is much less, and the quality of the fits is better, which indicates that the one-site model gives a good representation of the data. Also, the lower-temperature data appear to show the effect of heterodyning, i.e., the effects of two static interactions occurring at two different sites, which are characterized by two sets of similar frequencies. To check this possibility we used a two-site model, which is a generalization of Eq. (1), and we were able to obtain satisfactory fits to the lower-temperature data. These fits yielded fundamental frequencies  $\omega_1$  for each of the two sites that differed by 5–10% from each other as well as from the one-site-fit values. Thus the actual situation at lower temperatures may be that the probe interacts with two (or perhaps several) chemical environments that are similar but not identical, which could result from point defects being present near some of the probes. Whereas, at temperatures above  $T_c$ , the two environments become chemically equivalent. The available data are not sufficiently detailed to either confirm or rule out this possibility.

Figures 4 and 5 summarize the parameters derived from the fits to the data for  $\text{LiNbO}_3$  and  $\text{LiTaO}_3$ , respectively. For  $\text{LiNbO}_3$ , neither the efg parameters  $V_{zz}$  and  $\eta$  nor the other parameters  $\delta$  and  $f_1$  change very much over the temperature range of the measurements. Moreover, the asymmetry parameter  $\eta$  remains significantly

larger than zero over this range. These values of  $\eta$ , which are accompanied by relatively large values of the line-shape parameter  $\delta$ , cannot be attributed to the effects of static, inhomogeneous line broadening alone. Static line broadening results when a distribution characterizes each of the interaction frequencies  $\omega_k$ , and the measured

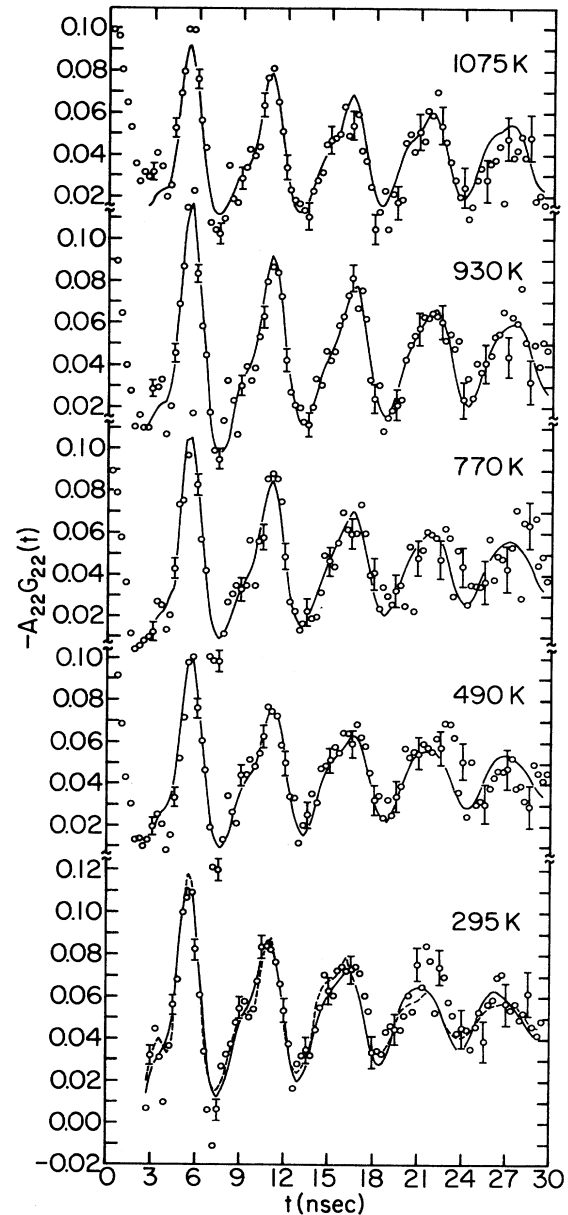


FIG. 2. Perturbation functions for a  $\text{LiNbO}_3$  ceramic sample. The solid lines represent least-squared fits of Eq. (1) to the experimental data. The dashed line represents a fit of a two-site model to the 295-K perturbation function. Data for  $t < 2$  nsec were excluded from the fits because the time distributions included irrelevant prompt coincidences that the detectors could not discriminate against. As part of the fitting process, Eq. (1) was convoluted with a Gaussian time-resolution function, which used a resolution of  $\approx 1$  nsec, full width at half maximum.

efg represents an average of the possible combinations of frequencies. The experimental consequence of these distributions is that a small but nonvanishing asymmetry is observed when the frequency distributions actually represent average axial symmetry at the probe site. The asymmetry-parameter values for ferroelectric  $\text{LiNbO}_3$ , which exceed 0.25 at the lower temperatures, indicate that a substantial breaking of the axial symmetry takes place. This effect cannot be attributed to static, inhomogeneous

line broadening. The values of the site-occupancy fraction  $f_1$  remain relatively constant over the entire temperature range. In addition, the large errors associated with most of the  $f_1$  values reflect the difficulties associated with obtaining fits that are good representations of the measured perturbation functions. For  $\text{LiTaO}_3$ , the efg component  $V_{zz}$  increases as temperature approaches the transition  $T_c$ ; and above the transition,  $V_{zz}$  decreases slowly. At temperatures well below  $T_c$ ,  $\eta$  is significantly larger than zero; and, as the temperature approaches  $T_c$ ,  $\eta$  decreases. At temperatures near and above  $T_c$ , the values of  $\eta$  are sufficiently close to zero to attribute the associated differences from zero to the effects of inhomogeneous linebroadening. The line-shape parameter  $\delta$  decreases at temperatures near and above  $T_c$ . This behavior is consistent with the decrease in the asymmetry parameter  $\eta$  over this temperature range. The  $f_1$  values for any specific sample remain relatively constant over the temperature range; and, as is the case for  $\text{LiNbO}_3$ , the errors associated with the  $f_1$  values obtained at lower temperatures are relatively large.

The magnitudes and the temperature dependences of  $V_{zz}$  and  $\eta$  measured by the  $^{181}\text{Ta}$  PAC probe in  $\text{LiTaO}_3$  differ markedly from the corresponding quantities measured by  $^{181}\text{Ta}$  ME<sup>20</sup> and NQR<sup>19</sup> spectroscopies at the Ta

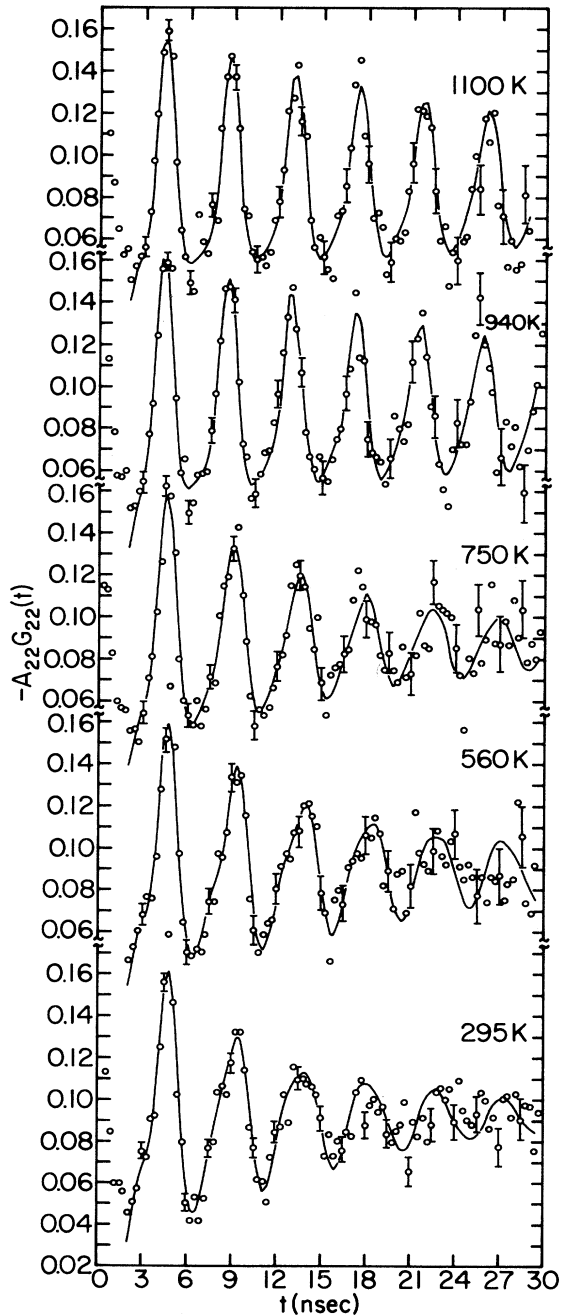


FIG. 3. Perturbation functions for a  $\text{LiTaO}_3$  ceramic sample. The solid lines represent fits which were obtained in a similar fashion to those shown in Fig. 2.

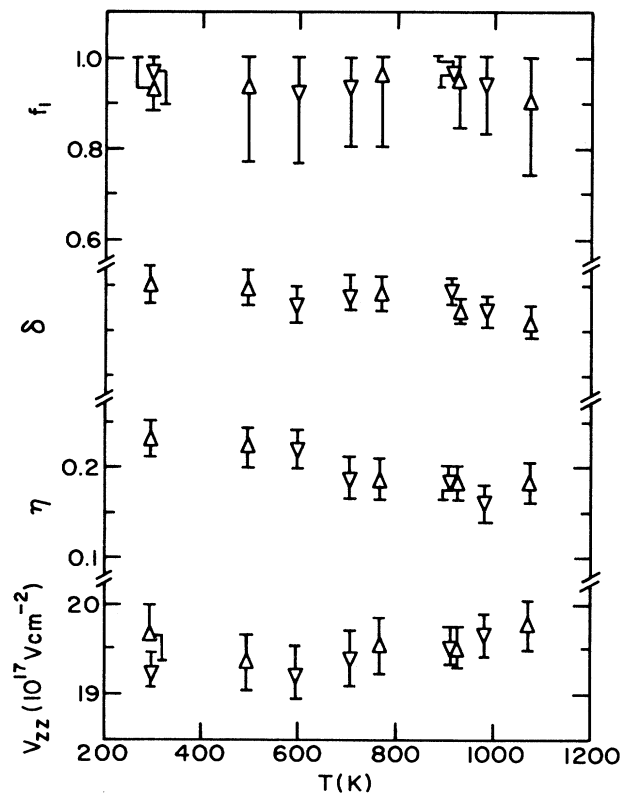


FIG. 4. Electric-field-gradient, line-shape, and site-occupancy-fraction parameters derived from fits to the  $\text{LiNbO}_3$  perturbation functions. The different types of data points represent different ceramic samples that were prepared and measured.

site in  $\text{LiTaO}_3$ . In particular, at laboratory temperature, at the  $^{181}\text{Ta}$  PAC probe site,  $V_{zz} = (22.8 \pm 0.4) \times 10^{17} \text{ V/cm}^2$  and  $\eta = 0.26 \pm 0.02$ , and at the Ta site,  $V_{zz} = 2.8 \times 10^{17} \text{ V/cm}^2$  and  $\eta = 0.1$ . At the  $^{181}\text{Ta}$  PAC probe site, as temperature increases from laboratory temperature to  $T_c$ ,  $V_{zz}$  increases and  $\eta$  decreases; whereas, at the actual Ta site, over the same temperature range,  $V_{zz}$  decreases and  $\eta$  increases. These differences indicate clearly that the  $^{181}\text{Ta}$  PAC probe site is not the Ta site in  $\text{LiTaO}_3$ . Moreover, as we discuss below, the  $^{181}\text{Ta}$  probe substitutes into the Li sites in  $\text{LiNbO}_3$  and  $\text{LiTaO}_3$ .

To investigate in more detail the behavior of the one-site-model parameters for  $\text{LiTaO}_3$  at temperatures near  $T_c$ , we performed an additional series of measurements on a different  $\text{LiTaO}_3$  sample. Figure 6 summarizes the

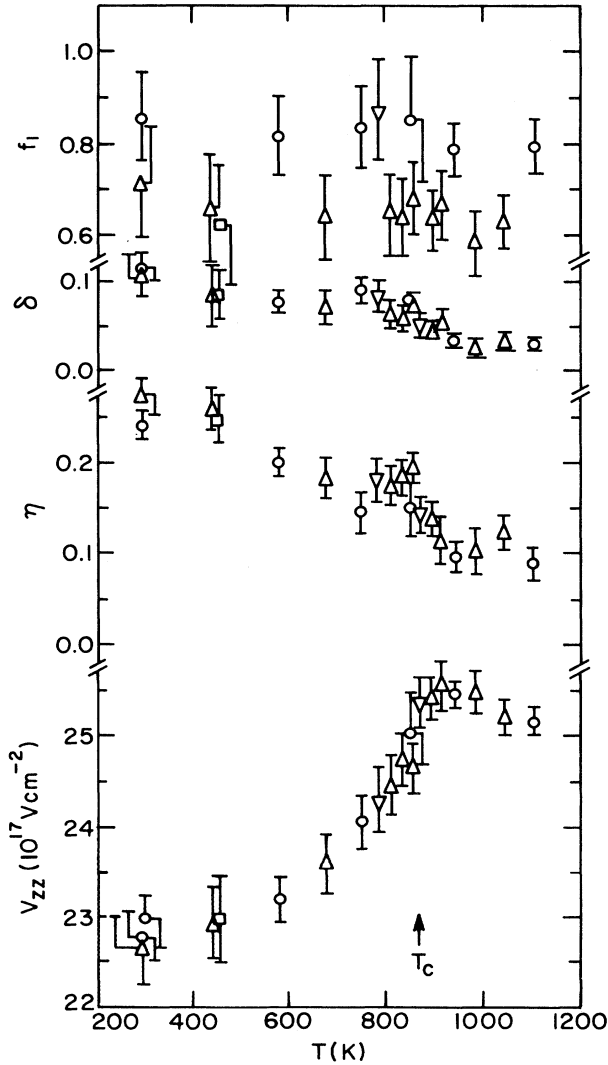


FIG. 5. Electric-field-gradient, line-shape, and site-occupancy-fraction parameters derived from fits to the  $\text{LiTaO}_3$  perturbation functions. The different types of data points represent several different ceramic samples that were prepared and measured.

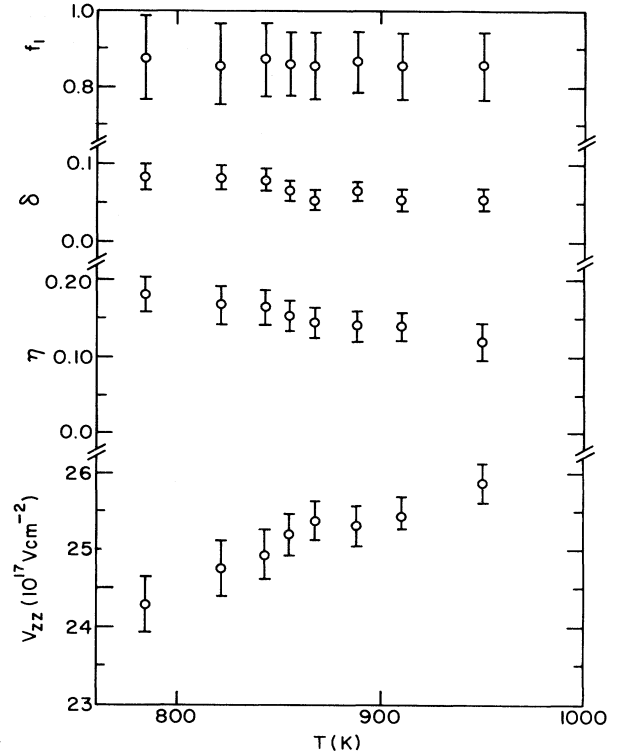


FIG. 6. Electric-field-gradient, line-shape, and site-occupancy-fraction parameters derived from fits to the  $\text{LiTaO}_3$  perturbation functions. This series of measurements was made on a single ceramic sample that was measured over a range of temperatures close to  $T_c$ . These values agree well with the values that Fig. 5 shows, which represent measurements on other  $\text{LiTaO}_3$  ceramic samples.

results. From heat capacity measurements, this ferroelectric-to-paraelectric transition has been established to be second order.<sup>17</sup> In addition, for crystals grown from the melt, the actual Curie temperature may range from 810 to 970 K depending on the growth conditions.<sup>17</sup> For ceramic samples we do not know how much variation in  $T_c$  from sample to sample to expect. Thus, we neither expect nor observe any significant inflections in the values of these parameters. Consistent with our expectations, as temperature increases, we do observe slow increases in  $V_{zz}$ , slow decreases in  $\eta$  and  $\delta$ , and no significant changes in  $f_1$ .

#### IV. DISCUSSION

##### A. Site substitution of the probe

At first consideration we would expect the  $^{181}\text{Hf} \rightarrow ^{181}\text{Ta}$  probe to substitute into the group-V sites in  $\text{LiNbO}_3$  and  $\text{LiTaO}_3$ , because the charge of the  $\text{Hf}^{4+}$  ion is close to those of the  $\text{Nb}^{5+}$  and  $\text{Ta}^{5+}$  ions and because these ions have similar ionic radii.<sup>23</sup> Also, we recently reported that the  $^{181}\text{Hf} \rightarrow ^{181}\text{Ta}$  probe substitutes unambiguously into the Nb sites in the ferroelastic ceramics  $\text{GdNbO}_4$  and  $\text{NdNbO}_4$ .<sup>24</sup> However, despite these simple considerations, Prieto *et al.*<sup>25</sup> showed, definitively, using

extended x-ray absorption fine-structure spectroscopy, that  $\text{Hf}^{4+}$  ions in concentrations of approximately 1 at. % substitute into the Li sites in single crystals of  $\text{LiNbO}_3$ . The Rutherford backscattering measurements of Rebouta *et al.*,<sup>26</sup> which they performed on Hf-doped single crystals of  $\text{LiNbO}_3$ , also show that  $\text{Hf}^{4+}$  ions substitute into Li sites. Abrahams and Marsh<sup>27</sup> performed a detailed x-ray diffraction study on  $\text{LiNbO}_3$  single crystals that had stoichiometric and congruently melting (defective) compositions. They determined the defect-structure composition to be  $(\text{Li}_{1-5x}\text{Nb}_{5x})\text{Nb}_{1-4x}\text{O}_3$ ,  $x = 0.0118$ . In crystals having this composition one Nb ion in approximately every three unit cells occupies a Li site and leaves a corresponding Nb site vacant. This result indicates that group-V antisite defects (e.g.,  $\text{Nb}_{\text{Li}}^{\cdot\cdot}$ , in Kröger-Vink notation), which should be similar in charge and size to the  $\text{Hf}^{4+}$  ions, are common in  $\text{LiNbO}_3$  and  $\text{LiTaO}_3$ . In addition, calculations for  $\text{LiNbO}_3$  crystals performed by Donnerberg *et al.*<sup>28</sup> indicate that  $\text{Nb}_{\text{Li}}^{\cdot\cdot}$  antisite defects are energetically favorable and that oxygen vacancies are not favorable. The defect-structure determination of Abrahams and Marsh<sup>27</sup> and the detailed calculations of Donnerberg *et al.*<sup>28</sup> are consistent with the experiments of Prieto *et al.*<sup>25</sup> and Rebouta *et al.*<sup>26</sup> Furthermore, the temperature dependences of  $V_{zz}$  and  $\eta$  measured by ME<sup>20</sup> and NQR<sup>19</sup> spectroscopies at the Ta site in  $\text{LiTaO}_3$  indicate that the  $^{181}\text{Hf} \rightarrow ^{181}\text{Ta}$  PAC experiment does not measure the efg at the Ta site in  $\text{LiTaO}_3$ . And, indeed, the PAC measurements represent the nuclear quadrupole interactions of  $^{181}\text{Ta}$  impurity nuclei at the Li sites in  $\text{LiNbO}_3$  and  $\text{LiTaO}_3$ .

### B. Temperature dependence of the efg in $\text{LiTaO}_3$

The efg parameters  $V_{zz}$  and  $\eta$ , which were measured at the Li site using the  $^{181}\text{Hf} \rightarrow ^{181}\text{Ta}$  PAC probe, exhibit unusual temperature dependences. The efg component  $V_{zz}$  increases with increasing temperature and reaches a maximum at a temperature near  $T_c$ . Above  $T_c$ ,  $V_{zz}$  decreases slowly. The asymmetry parameter decreases with temperature and reaches values reasonably close to zero at temperatures above  $T_c$ . According to the diffraction-derived structure,<sup>2</sup> the Li site lies on the  $c$  axis, which is an axis of threefold rotational symmetry. For this reason, if the efg axes were parallel to the crystallographic axis, then the efg would have axial symmetry and the asymmetry parameter would vanish. Clearly  $\eta$  is nonzero at temperatures well below  $T_c$ . Thus the axial symmetry at the Li site is being broken.

Group-V antisite defects,  $\text{Ta}_{\text{Li}}^{\cdot\cdot}$  in this case, could contribute to breaking the axial symmetry at the Li sites, especially since the nonstoichiometric composition (of  $\text{LiNbO}_3$ , strictly speaking) is known to contain sufficient numbers of these defects<sup>27</sup> to be measurable. The continuous change in  $\eta$  with increasing temperature suggests that the defects that produce the asymmetry in the efg are mobile. Because  $\text{Li}^+$  ions are much more mobile in the  $\text{LiTaO}_3$  structure, it is possible that an order-disorder mechanism that involves  $\text{Li}^+$  ions contributes more to breaking the efg symmetry than does the group-V antisite

defect formation mechanism.

We can understand this symmetry breaking mechanism by considering the order-disorder model proposed by Birnie.<sup>29-31</sup> The diffraction-derived  $\text{LiTaO}_3$  structure, which Ref. 1 illustrates well, is composed of columns of oxygen octahedra that are oriented along the  $c$ -axis direction. The octahedra are filled by metal ions in the sequence: Ta-Li-vacancy-Ta-Li-vacancy, etc. In this structure, as the calculations of Donnerberg *et al.*<sup>23</sup> confirm, Li ions readily form interstitials that occur when a  $\text{Li}^+$  ion jumps from a normally occupied Li site in an oxygen octahedron to a normally vacant octahedron. In the diffraction-derived structure, *no* interstitials exist. In the structure of the ordered ferroelectric phase, interstitials exist, but the number of  $\text{Li}^+$  ions in the normal Li sites (octahedra) outnumbers the interstitials. In the structure of the disordered, paraelectric phase,  $\text{Li}^+$  ions occur with equal probability in either the normal Li sites or the Li interstitial sites. Interactions between Li and Ta ions produce dipoles. The dipoles produced by normal-site Li ions and Ta ions are oriented in a particular direction, but those produced by interstitial Li ions and Ta ions are oriented in the opposite direction. The spontaneous polarization arises in the ferroelectric phase because the occupancy of a normal Li site by a  $\text{Li}^+$  ion is favored. Similarly the spontaneous polarization vanishes in the paraelectric phase because the Li site occupancies have equal probability.

In the context of the efg asymmetry, we recognize that, at temperatures well below  $T_c$ , the asymmetry should vanish if all of the  $\text{Li}^+$  ions were to occupy normal Li sites, i.e., if the diffraction-derived structure were an accurate representation of the crystal. The unequal distribution of  $\text{Li}^+$  ions between normal and interstitial Li sites, therefore, must be breaking the axial symmetry associated with the diffraction-derived structure. Furthermore, the near-vanishing asymmetry observed at temperatures above  $T_c$  implies that the distribution of ionic charge, i.e.,  $\text{Li}^+$  ions in interstitial sites, which we presume breaks the efg axial symmetry at temperatures well below  $T_c$ , becomes spatially averaged. That is, equal occupancy of the normal and the interstitial Li sites (by  $\text{Li}^+$  ions) gives essentially zero asymmetry of the efg. Thus, Birnie's model<sup>29-31</sup> explains qualitatively the non-vanishing asymmetry of the Li-site efg.

The order-disorder mechanism qualitatively explains the temperature dependence of the line-shape parameter  $\delta$ . The probe environment in the crystal consists of a  $^{181}\text{Ta}^{5+}$  ion at a Li site. The nearest interstitial Li sites may be occupied by either  $\text{Li}^+$  ions or  $\text{Ta}_{\text{Li}}^{\cdot\cdot}$  antisite defects, or they may be vacant. The occupation of interstitial Li sites means that some of the nearest normal Li sites are vacant, which could produce "defective" probe environments. Because the interstitial Li sites in the structure are ordered with respect to the normal Li sites, we expect the interstitial sites occupied by  $\text{Li}^+$  ions to give rise to a well-defined but asymmetric efg. But, the experimental measurement represents an average of this asymmetric efg, the normal symmetric efg, and efgs that arise from defective probe environments. At temperatures well below  $T_c$ , the  $\delta$  values are large,  $\delta \approx 0.1$ , and

the simple line-broadening factor  $\exp(-\frac{1}{2}\delta\omega_k t_i)$  in Eq. (1) does not completely account for the observed line broadening. Whereas, at temperatures above  $T_c$ , the  $\delta$  values are systematically lower and the quality of the fits is better. Thus, the line shapes of the perturbation functions measured above  $T_c$  are consistent with the spatial averaging of the probe environment that the order-disorder model implies. The line shapes of the perturbation functions measured well below  $T_c$  are not inconsistent with the superposition of the several types of probe environments that the model suggests.

At temperatures below  $T_c$ , the magnitude of the efg component  $V_{zz}$  increases as temperature approaches  $T_c$ ; and above  $T_c$ ,  $V_{zz}$  decreases slowly. This result is unexpected and anomalous. From our investigations<sup>32</sup> and the investigations of others<sup>33</sup> on  $ABO_3$  ferroelectric perovskites such as  $BaTiO_3$  and  $PbTiO_3$ , we know that  $V_{zz}$  and the spontaneous polarization  $P_s$  both decrease (although perhaps not at the same rate) as temperature approaches  $T_c$ . Both of these effects can be explained by considering the corresponding changes in the crystal structures. The  $ABO_3$  perovskite structures of  $BaTiO_3$  and  $PbTiO_3$  change from tetragonal to cubic symmetry during the ferroelectric-to-paraelectric transitions. At laboratory temperature, the  $c/a$  lattice parameter ratio is 1.01 for  $BaTiO_3$  and 1.06 for  $PbTiO_3$ . The associated differences in the  $V_{zz}$  and  $P_s$  values for these two compounds correlate qualitatively with the differences in the corresponding  $c/a$  ratios. As temperature increases, the  $c/a$  ratios approach unity as the structures of both of these compounds become more symmetric and the corresponding values of  $V_{zz}$  and  $P_s$  decrease and approach zero. The values of the asymmetry parameter  $\eta$  do not change much with temperature. Although we suggested that both displacive and order-disorder effects give rise to the Ti site efgs in  $BaTiO_3$  and  $PbTiO_3$ ,<sup>32,33</sup> we can describe the decrease of  $V_{zz}$  as temperature approaches  $T_c$  in the context of either mechanism, in which the crystal becomes more symmetric as temperature increases. Similarly, in the context of either mechanism, the  $LiTaO_3$  structure becomes more symmetric and  $P_s$  decreases as temperature approaches  $T_c$ . But, over the same temperature range,  $V_{zz}$  increases instead of decreasing. Unlike the ferroelectricity in  $ABO_3$  perovskites such as  $BaTiO_3$  and  $PbTiO_3$ , the temperature dependence of  $V_{zz}$  is not strongly coupled to the temperature dependence of  $P_s$ . Moreover, unlike the strong correlation between  $V_{zz}$  and  $P_s^2$  that Yeshurun, Havlin, and Schlesinger observed<sup>34</sup> and interpreted<sup>35</sup> at temperatures well below  $T_c$  in the antiferroelectric perovskite,  $PbHfO_3$ , the correlation in  $LiTaO_3$  may be between  $\eta$  and  $P_s$ , i.e.,  $\eta$  may be coupled to the order parameter for the transition. These interesting results indicate that a more-detailed, quantitative model is required to explain the temperature dependence of the magnitude and the asymmetry of the Li-site efg in  $LiTaO_3$ .

## V. CONCLUSIONS

Well-defined, static nuclear-quadrupole interactions were measured at the Li sites in  $LiNbO_3$  and  $LiTaO_3$  using the  $^{181}\text{Hf} \rightarrow ^{181}\text{Ta}$  PAC probe. At temperatures well below  $T_c$ , the measured perturbation functions show extensive line broadening and the derived efgs show anomalous asymmetries that are not predicted from the diffraction-derived structure. At temperatures above  $T_c$  (for  $LiTaO_3$ ), the efg asymmetry is nearly zero, and the line broadening decreases. Birnie's order-disorder model<sup>29-31</sup> can be used qualitatively to account for the temperature dependences of the asymmetry and the line broadening. These effects can be attributed to primarily to Li ions that occupy normally vacant sites in the crystal structures.

In  $LiTaO_3$ , the efg component  $V_{zz}$  increases as temperature approaches  $T_c$ , even through the corresponding spontaneous polarization  $P_s$  decreases. The anticorrelation of the  $V_{zz}$  temperature dependence with that for  $P_s$  suggests that  $V_{zz}$  is not strongly coupled to the order parameter for the transition, and this relationship is unlike the strong correlation observed between  $V_{zz}$  and  $P_s^2$  for  $PbHfO_3$ . Instead the asymmetry parameter  $\eta$  may be coupled to the order parameter for the transition.

At temperatures in the vicinity of  $T_c$ , the smooth changes of  $V_{zz}$ ,  $\eta$ ,  $\delta$  with temperature are consistent with the well-established second-order character of the transition. The temperature dependences of  $V_{zz}$  and  $\eta$  measured by the  $^{181}\text{Ta}$  PAC probe at the Li site in  $LiTaO_3$  complement the corresponding information measured earlier by  $^{181}\text{Ta}$  ME and NQR spectroscopies. To exploit this information, a more detailed model that can be used to explicitly calculate accurate efgs at both the Li and the Ta sites in  $LiNbO_3$  and  $LiTaO_3$  is needed.

## ACKNOWLEDGMENTS

We thank Professor Dunbar P. Birnie III of the University of Arizona for introducing us to his order-disorder model and for critically reading this manuscript. His detailed comments and suggestions were extremely helpful. We thank Professor Robert L. Rasera of the University of Maryland, Baltimore County, for his insightful comments on this investigation. We acknowledge Professor Stewart K. Kurtz of the Materials Research Laboratory, for much encouragement and many helpful comments. We thank Dr. Ian D. Williams of the Materials Research Laboratory, who shared many insights into the crystal chemistry of group-IV and -V elements with us. We gratefully acknowledge support from the Office of Naval Research (Grant No. N00014-90-J-4112).

- \*Permanent address: Babcock & Wilcox Co., Lynchburg, VA 24506.
- <sup>1</sup>S. C. Abrahams, J. M. Reddy, and J. L. Bernstein, *J. Phys. Chem. Solids* **27**, 997 (1966).
- <sup>2</sup>S. C. Abrahams and J. L. Bernstein, *J. Phys. Chem. Solids* **28**, 1685 (1967).
- <sup>3</sup>For a brief review of the earlier work, see M. E. Lines and A. M. Glass, *Principles and Applications of Ferroelectrics and Related Materials* (Clarendon Press, Oxford, 1977), pp. 226–280.
- <sup>4</sup>For a more-recent review, see A. M. Prokhorov and Yu. S. Kuz'minov, *Physics and Chemistry of Crystalline Lithium Niobate* (Adam Hilger, New York, 1990).
- <sup>5</sup>G. Burns, *Phys. Rev.* **127**, 1193 (1962).
- <sup>6</sup>G. E. Peterson, P. M. Bridenbaugh, and P. Green, *J. Chem. Phys.* **46**, 4009 (1967).
- <sup>7</sup>G. E. Peterson and P. M. Bridenbaugh, *J. Chem. Phys.* **48**, 3402 (1968).
- <sup>8</sup>G. E. Peterson and J. R. Carruthers, *J. Solid State Chem.* **1**, 98 (1969).
- <sup>9</sup>J. R. Carruthers, G. E. Peterson, M. Grasso, and P. M. Bridenbaugh, *J. Appl. Phys.* **42**, 1846 (1971).
- <sup>10</sup>G. E. Peterson and A. Carnevale, *J. Chem. Phys.* **56**, 4848 (1972).
- <sup>11</sup>D. C. Douglass and G. E. Peterson, *J. Am. Ceram. Soc.* **69**, 48 (1986).
- <sup>12</sup>D. C. Douglass, G. E. Peterson, and V. J. McBrierty, *Phys. Rev. B* **40**, 10 694 (1989).
- <sup>13</sup>G. E. Peterson, J. R. Carruthers, and A. Carnevale, *J. Chem. Phys.* **53**, 2436 (1970).
- <sup>14</sup>T. K. Halstead, *J. Chem. Phys.* **53**, 3427 (1970).
- <sup>15</sup>D. Slotfeldt-Ellingsen and B. Pedersen, *Phys. Status Solidi A* **24**, 191 (1974).
- <sup>16</sup>B. T. Matthias and J. P. Remeika, *Phys. Rev.* **76**, 1886 (1949).
- <sup>17</sup>A. M. Glass, *Phys. Rev.* **172**, 564 (1968).
- <sup>18</sup>E. Schempp, G. E. Peterson, and J. R. Carruthers, *J. Chem. Phys.* **53**, 306 (1970).
- <sup>19</sup>A. P. Zhukov, L. V. Soboleva, L. M. Belyaev, and A. F. Volkov, *Ferroelectrics* **21**, 601 (1978).
- <sup>20</sup>M. Löhnert, G. Kaindl, G. Wortmann, and D. Salomon, *Phys. Rev. Lett.* **47**, 194 (1981).
- <sup>21</sup>G. L. Catchen, L. H. Menke, Jr., K. Jamil, M. Blaszkiwicz, and B. E. Scheetz, *Phys. Rev. B* **39**, 3826 (1989).
- <sup>22</sup>See, for example, G. L. Catchen, *Hyperfine Interactions* **52**, 65 (1989); G. L. Catchen, *J. Mater. Educ.* **12**, 253 (1990).
- <sup>23</sup>O. Muller and R. Roy, *The Major Ternary Structural Families* (Springer-Verlag, Berlin, 1974), pp. 5–7.
- <sup>24</sup>G. L. Catchen, I. D. Williams, D. M. Spaar, S. J. Wukitch, and J. M. Adams, *Phys. Rev. B* **43**, 1138 (1991).
- <sup>25</sup>C. Prieto, C. Zaldo, P. Fessler, H. Dexpert, J. A. Sanz-Garcia, and E. Diéquez, *Phys. Rev. B* **43**, 2594 (1991).
- <sup>26</sup>L. Rebouta, J. C. Soares, M. F. Dá Silva, J. A. Sanz-Garcia, E. Diequez, and F. Agulló-López, *Nucl. Instrum. Methods B* **50**, 428 (1990).
- <sup>27</sup>S. C. Abrahams and P. Marsh, *Acta Crystallogr. B* **42**, 61 (1986).
- <sup>28</sup>H. Donnerberg, S. M. Tomlinson, C. R. A. Catlow, and O. F. Schirmer, *Phys. Rev. B* **40**, 11 909 (1989).
- <sup>29</sup>D. P. Birnie III, *J. Mater. Res.* **5**, 1933 (1990).
- <sup>30</sup>D. P. Birnie III, *J. Am. Ceram. Soc.* **74**, 988 (1991).
- <sup>31</sup>D. P. Birnie III, *J. Appl. Phys.* **69**, 2485 (1991).
- <sup>32</sup>G. L. Catchen, S. J. Wukitch, D. M. Spaar, and M. Blaskiewicz, *Phys. Rev. B* **42**, 1885 (1990).
- <sup>33</sup>For a review of PAC measurements performed on  $ABO_3$  perovskites, see G. L. Catchen, S. J. Wukitch, E. M. Saylor, W. Huebner, and M. Blaszkiwicz, *Ferroelectrics* **117**, 175 (1991).
- <sup>34</sup>Y. Yeshurun, Y. Schlesinger, and S. Havlin, *J. Phys. Chem. Solids* **40**, 231 (1979).
- <sup>35</sup>Y. Yeshurun, S. Havlin, and Y. Schlesinger, *Solid State Commun.* **27**, 181 (1978).